american physiological society

JNP JOURNAL OF NEUROPHYSIOLOGY

J Neurophysiol 133: 727–741, 2025.
First published January 20, 2025; doi:10.1152/jn.00246.2024

RESEARCH ARTICLE

Control of Movement

Changes in thoracic erector spinae regional activation during postural adjustments and functional reaching tasks after spinal cord injury

Joeri F. L. van Helden,[1] Hélio V. Cabral,[2] Emma Alexander,[3] Paul H. Strutton,[4] Eduardo Martinez-Valdes,[1] Deborah Falla,[1] Joy Roy Chowdhury,[5] and Shin-Yi Chiou[1]

[1]*Centre of Precision Rehabilitation for Spinal Pain (CPR Spine), School of Sport, Exercise and Rehabilitation Sciences, College of Life and Environmental Sciences, University of Birmingham, Birmingham, United Kingdom;* [2]*Department of Clinical and Experimental Sciences, Università degli Studi di Brescia, Brescia, Italy;* [3]*The Royal London Hospital, Barts Health NHS Trust, London, United Kingdom;* [4]*Department of Surgery & Cancer, Faculty of Medicine, Imperial College London, London, United Kingdom; and* [5]*Midland Centre for Spinal Injuries, The Robert Jones and Agnes Hunt Orthopaedic Hospital NHSFT, United Kingdom*

Abstract

Many individuals with incomplete spinal cord injury (SCI) exhibit reduced volitional control of trunk muscles, such as impaired voluntary contractions of the erector spinae (ES), due to damage to the neural pathways regulating sensorimotor function. Studies using conventional bipolar electromyography (EMG) showed alterations in the overall, or global, activation of the trunk muscles in people with SCI. However, how activation varied across specific regions within the ES, referred to as regional activation, remains unknown. The aim of the study was to investigate the regional distribution of the ES activity below the level of injury in individuals with incomplete SCI during postural tasks and multidirectional reaching tasks using high-density EMG. Twenty-one individuals with incomplete SCI and age-matched controls were recruited. The EMG amplitude of the thoracic ES and displacement of the arm, trunk, and center of pressure were recorded during the tasks. Activation was more in the lower region of the ES in individuals with SCI than in the controls during the postural tasks. In addition, activation was limited to a small area of the ES during the reaching tasks. The EMG amplitude was greater during reaching forward than returning to the upright posture in the controls; however, this phase-dependent difference in the EMG amplitude was not present in individuals with SCI. Our findings demonstrate changes in regional activation of the thoracic ES during postural and reaching tasks, likely reflecting injury-induced changes in selective neural control to activate residual muscle fibers of the ES for postural control and function after SCI.

NEW & NOTEWORTHY We demonstrate that individuals with chronic incomplete spinal cord injury (SCI) recruit lower part of the thoracic erector spinae (ES) for postural control of the trunk. We also show that activation was restricted in a smaller part of the ES, and the discrete control of the ES was lost during functional reaching movements in individuals with SCI. Our study provides evidence of alterations in neural control between vertebral levels in individuals with SCI.

high-density surface electromyography; motor control; muscle recruitment; neuromuscular function; postural control

INTRODUCTION

Damage to the spinal cord can affect synaptic input from the descending motor axons to the motor neurons in the spinal cord below the level of injury (1, 2), resulting in regional changes in activation of the muscles and impaired voluntary movements (3, 4). Consequently, individuals with spinal cord injury (SCI) develop new motor control strategies using the muscles with intact or partial sensorimotor function (5, 6). After SCI, the ability to voluntarily activate trunk muscles, such as erector spinae (ES), decreased (7). This impaired volitional control of trunk muscles can reduce individuals' ability to carry out activities of daily living, such as reaching for an object and maintaining

Correspondence: S.-Y. Chiou (s.chiou@bham.ac.uk).
Submitted 13 June 2024 / Revised 13 August 2024 / Accepted 16 January 2025

0022-3077/25 Copyright © 2025 The Authors. Licensed under Creative Commons Attribution CC-BY 4.0.
Published by the American Physiological Society.

Downloaded from journals.physiology.org/journal/jn at Imperial Col London (2A0C:5BC0:0040:1008:1A60:24FF:FEA6:CAE5) on July 16, 2025.

an upright seated posture (5, 8). The erector spinae (ES) is a key muscle group for maintaining an upright posture (9, 10), providing a stable base from which the upper extremities can move functionally such as during forward and lateral reaching (5). Research has shown task-specific motor unit activity of the ES between vertebral levels during functional tasks in healthy adults (11, 12), suggesting different motoneuronal pools innervating the ES between spinal segments and that task-specific synaptic input to those motoneuronal pools for control of ES activity. Following SCI, neural reorganization in the spinal cord can alter the synaptic input to the motor neurons below the level of injury, with some muscle fibers losing activation capacity while others retain supraspinal influence (13, 14). This can lead to a redistribution of activation toward the residual or reinnervated muscle fibers, resulting in changes in spatial activation of the ES. Studies have reported changes in trunk muscle activation during functional tasks after SCI, such as decreased ES activity (15, 16) and altered trunk muscle activity for anticipatory postural adjustments and compensatory postural adjustments (APAs and CPAs) in postural control (17). For example, people with chronic SCI showed delayed ES activity during APAs in a rapid shoulder flexion task (7) and demonstrated increased ES activity during CPAs when performing manual wheelchair propulsion (18). Although those studies demonstrated altered temporal activation of the ES after SCI, it remains unknown whether spatial activation of the ES occurs across several spinal segments during voluntary motor tasks after SCI. Understanding changes in spatial distribution of the ES will provide insights into optimization of the use of residual or reinnervated muscle fibers to maintain postural stability and perform motor tasks after SCI. This new knowledge may inform treatment plans to improve voluntary movement of the trunk and postural control in individuals with SCI.

High-density surface EMG (HDEMG) provides a topographical representation of muscle activity, allowing the identification of activation across specific regions within a muscle, referred to as regional activation, which can be used to indicate synaptic input to the specific regions of the muscle (19–21). Using HDEMG, previous studies reported a shift in ES activity along the spinal column (i.e., cranio-caudal shift) during voluntary motor tasks, such as trunk flexion-extension (e.g., rowing, forward bending) and lifting (22–24). The cranio-caudal shift of activation of the ES may be related to the architecture of the muscle fibers and the innervation zones of the ES that are predominantly distributed in a narrow band along the muscle fibers in the cranio-caudal direction (25, 26). Damage to the spinal cord and spinal nerves can change the innervation to the ES and thereby likely lead to changes in activation in the direction along the muscle fiber, i.e., a cranio-caudal shift in activation. Hence, the aim of the study was to characterize the regional activation of thoracic ES during voluntary motor tasks in adults with chronic incomplete SCI using HDEMG and to compare that with age-matched controls without an SCI. We hypothesized that individuals with chronic incomplete SCI would demonstrate different regional activation of the ES along the muscle fiber direction, i.e., in the cranio-caudal direction, compared with control individuals.

MATERIALS AND METHODS

Participants

An a priori power calculation drawn from a previous study (27) and our unpublished data suggested a sample size of 21 individuals in each group was sufficient to detect a between-group difference for the root-mean-square amplitudes of the ES activity in forward reaching with 90% power and a 5% level of significance. Twenty-one individuals with incomplete SCI were recruited (17 men; 15 right side least affected; age 55.2 yr, SD 12.5; various races) from the Robert Jones and Agnes Hunt Orthopaedic Hospital in Oswestry, UK, and from local SCI charities between 2019 and 2022. Individuals were tested in the laboratories at the University of Birmingham. Inclusion criteria were *1*) having a stable, incomplete cervical or thoracic SCI, classified using the International Standards for Neurological Classification of Spinal Cord Injury examination and by the American Spinal Cord Injury Association Impairment Scale (AIS), *2*) time since injury more than 12 mo, *3*) being able to voluntarily move the upper extremities to perform the motor tasks, described in the *Experimental Procedures*, *4*) being able sit independently for 30 s, and *5*) aged 18 yrs or above. Screening against the inclusion criteria was conducted in the laboratory to ensure that participants met the eligibility requirements. For the control group, 21 age-matched adults without SCI were recruited (7 men; 18 right-handed; age 53.5 yr, SD 13.2, various races). Ethics approval was obtained from the Health Research Authority West Midlands - Edgbaston Research Ethics Committee (21/WM/0047) and was performed in accordance with the principles outlined in the Declaration of Helsinki. All participants provided written informed consent before any data collection.

Experimental Procedures

All participants undertook a rapid shoulder flexion (RSF) task (28), an external perturbation task, and multidirectional reaching tasks. The RSF and external perturbation tasks were selected to investigate ES activation in different types of postural adjustments. The RSF is a self-initiated perturbation and commonly used to study APAs. The external perturbation task is an externally induced perturbation and can be used to evaluate both APAs and CPAs. The multidirectional reaching task was selected to evaluate ES activation during dynamic sitting balance (29). Those tasks are functionally different and were chosen to allow for evaluation of a diverse role of the ES in activities of daily living. Participants sat on a custom-made chair (without back support), with an embedded force plate (BTS P6000, BTS Bioengineering Corp, Quincy, MA), feet flat on the floor and hips and knees at 90°. Participants were instructed to sit as upright as possible without using their arms for support or balance on the chair. They practiced the tasks under supervision to ensure that they performed them correctly and safely. Throughout data collection, participants were constantly reminded to avoid using their other arm for stability; a researcher always remained close to ensuring safety in case of any loss of balance. Only successful trials were included in the data analysis.

For the RSF task (Fig. 1*A*), participants were asked to raise both arms from the sides to the front at ~90° as fast as possible

Downloaded from journals.physiology.org/journal/jn at Imperial Col London (2A0C:5BC0:0040:1008:1A60:24FF:FEA6:CAE5) on July 16, 2025.

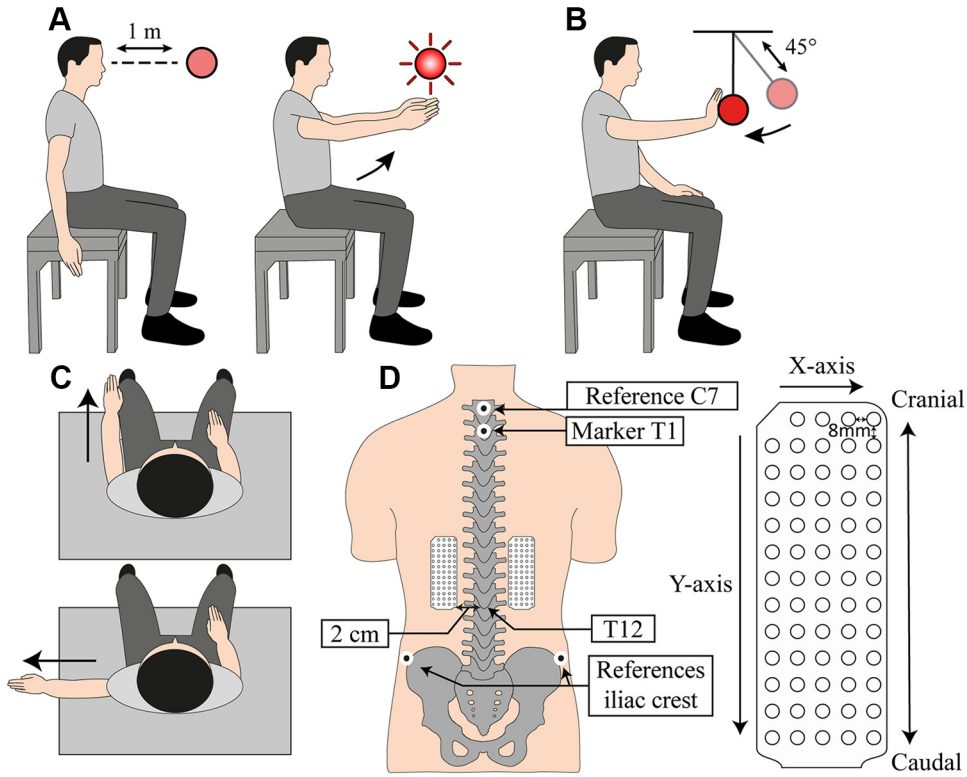


Figure 1. Experimental setup. *A*: rapid shoulder flexion. Participants flexed their shoulders bilaterally as quickly as possible in response to a visual cue. *B*: external perturbation task. A weight ~5% of the participant's body mass was pulled back to a 45-deg angle and released to the participant's extended arm. *C*: forward reaching (*top*) and lateral reaching (*bottom*) tasks. Participants reached with their dominant or less affected arm as far as possible at their comfortable pace. *D*: high-density surface electromyography grids were placed in parallel with the thoracic spine over the erector spinae, with the bottom of the grids placed 2 cm laterally from the 12th thoracic spinous process. Reflective markers were placed bilaterally over the ulnar styloid processes and over the 1st thoracic spinous process.

in response to a LED light placed ~1 m distance at eye level; this was repeated five times. Before each visual cue, a verbal warning cue was given by the experimenter, with a random interval of 1–3 s between the warning and visual cue. For the external perturbation task (Fig. 1*B*), we used a previously described method using a pendulum involving a weight of 5% of the body mass of the individuals being released from a 45° angle toward the extended arm of the participants (less affected arm for participants with SCI based on the manual muscle testing, and the dominant arm for the controls) to create a perturbation to the body (30). Participants were seated upright and held their arm in 90° of shoulder flexion; the other arm rested on their thigh. They were instructed to maintain their balance, not allowing the weight to move them. The task was repeated five times. For the multidirectional reaching tasks (Fig. 1*C*), participants were asked to sit in an upright position and move the trunk and use the less affected arm to reach forward and to the side as far as possible without losing balance five times. They were instructed to rest their other arm on their thighs and not to use it for balance. If a participant began using the other arm for compensation or balance during reaching, the trial was discarded.

Data Acquisition

HDEMG.

Muscle activity was recorded bilaterally from thoracic ES using two semidisposable HDEMG grids (GR08MM1305, OT Bioelettronica, Turin, Italy). The electrode grids consisted of 64 electrodes arranged in 13 rows by five columns, with one missing channel in the top left corner (see Fig. 1*D*; 1 mm electrode diameter, 8 mm interelectrode distance). An adhesive foam (KIT08MM1305, OT Bioelettronica, Turin, Italy) was attached to the grid and its cavities were evenly filled with conductive paste (AC Cream, Spes Medica, Genoa, Italy). Before placement of the electrode grids, the skin was shaved, gently abraded with a paste (Nuprep Skin Prep Gel, Weaver and Company, CO), and cleaned with alcohol-based skin wipes (GAMA Healthcare, Hertfordshire, UK) to remove any residue from the paste. Grids were placed over the thoracic ES in parallel with the thoracic spine, with the bottom edge of the grids placed 2 cm from each lateral side of the 12th thoracic spinous process, and the top edge extended in the cranial direction, approximating the 8th thoracic spinous process (Fig. 1*D*). Reference electrodes (Ambu WhiteSensor WS, Ballerup, Denmark; 36 mm × 40 mm) were placed over the 7th cervical spinous process and bilaterally over the iliac crests. Two bipolar electrodes (Ambu WhiteSensor WS, Ballerup, Denmark; 36 mm × 40 mm; 20 mm interelectrode distance) were placed bilaterally over the anterior deltoid (AD) to measure the onset of muscle activity during the RSF task. Any loose wires were taped to the participant. HDEMG was recorded in monopolar mode with an amplifier (150 V/V gain; Quattrocento, OT Bioelettronica, Turin, Italy) and digitized at 2,048 Hz using a 16-bits A/D converter (10–500 Hz bandpass filter with a 3 dB cut off frequency, input resistance $>10^{11}$ Ω, common mode rejection ratio >95 dB, noise level referred to input <4 μV). All data were collected using the OT Biolab software (OT Bioelettronica, Turin, Italy) and stored in a local computer for post-processing purposes.

Kinematics.

A 3-D optical motion capture system with eight cameras (Smart-DX 6000, BTS Bioengineering Corp, Quincy, MA) and the force plate were used to record motion and center of pressure (CoP), respectively, both sampled at 250 Hz. Reflective markers were placed bilaterally over the ulnar

Downloaded from journals.physiology.org/journal/jn at Imperial Col London (2A0C:5BC0:0040:1008:1A60:24FF:FEA6:CAE5) on July 16, 2025.

styloid processes and over the 1st thoracic spinous process to measure reaching distance and trunk displacement, respectively. Prior work has shown the movement of the lower cervical/higher thoracic spine can provide useful information relating to the movement of the pelvis in reaching (31). The marker's reflections were used to calculate trunk displacements in all tasks, to identify the moment of impact in the external perturbation task, and to calculate reaching distance in the multidirectional reaching tasks (31). A transistor-to-transistor logic device with an output of 5 V was used to synchronize EMG data with motion data.

Data Processing

All data processing was performed in MATLAB 2021a (MathWorks, Natick, MA). Signals were first band-pass filtered (20–350 Hz; second-order Butterworth filter) (32, 33). Monopolar EMG signals from HDEMG were then visually inspected to identify low-quality channels due to movement artifacts or power line interference. Low-quality channels were replaced with the linear interpolation of the neighboring channels when the following criteria were fulfilled: at least two high-quality channels in neighboring rows surrounding the low-quality channel and one high-quality channel above or under the low-quality channel had to be available to perform the linear interpolation. If the criteria were not met, the channel was removed in the second visual inspection. Differential signals were then calculated as the algebraic difference between monopolar signals detected by consecutive rows of electrodes. A second visual inspection was then carried out on the differential channels to further identify low-quality channels (4.44% of channels removed across participants, grids, and tasks). For each repetition of each task, the root mean square (RMS) amplitude was calculated for each of the 59 single-differential channels, providing topographical maps of thoracic ES EMG amplitude. Active channels were identified as those presenting an RMS amplitude higher than 70% of the maximum RMS amplitude across the grid. The 70% amplitude threshold was selected because it has been shown to provide a robust identification of active portions of the muscle (34). To characterize the spatial distribution of ES activity, i.e., the regional activation of the ES, the centroid coordinates were calculated as the weighted average of active channels across columns (mediolateral; x-axis) and rows (cranio-caudal; y-axis) to determine the center of the EMG amplitude map.

For the kinematic data, displacement of the trunk and wrist markers and the CoP were calculated by subtracting the maximum anterior/posterior (forward reaching) or medial/lateral (lateral reaching) value from the minimum value in each repetition. Total trajectory of the CoP was calculated as the sum of the absolute difference in the anterior-posterior (A-P) and medio-lateral (M-L) planes. Angular velocity of the movement of the dominant arm or less affected arm during the RSF task was calculated based on the wrist marker (35). For all HDEMG and kinematic parameters, the mean was calculated across repetitions.

RSF task.

The onset of the rise in EMG activity of AD and ES was determined as the point where rectified EMG traces exceeded 3 SD of the mean EMG amplitude in a window of 100 ms before the visual cue (36, 37). APAs, differences in EMG onset between AD and ES, were calculated by subtracting EMG onset of AD from ES. To quantify muscle activity and movement during APAs, HDEMG and the CoP in the A-P direction were analyzed from the onset of ES to +50ms (38). Furthermore, to understand muscle activity and movement during the entire shoulder flexion phase of the RSF task, data were analyzed from the onset of movement of the wrist marker of the dominant or less affected side to the highest vertical displacement peak of the marker in which the shoulders were in maximal flexion.

External perturbation task.

In each repetition, the first displacement of the wrist marker, which showed a clear peak in the motion data, was used to register the moment of the impact of the perturbation. To analyze the onset of the ES contralateral to the extended arm, EMG was rectified, and linear envelopes were created with a 20-Hz low-pass Butterworth filter. The EMG onset was defined as the point when the increase in EMG amplitude was more than 2 SD of the mean EMG value in a window between 500 ms and 400 ms before the impact (39). APAs and CPAs were derived from the moment of impact as the time windows of −100 ms to 50 ms and 50 ms to 200 ms, respectively (39), that were subsequently used to analyze EMG of the ES contralateral to the extended arm and the CoP data.

Multidirectional reaching tasks.

Using the maximal reaching distance point, each repetition was separated into reaching (forward/lateral) and returning (returning to initial position) phases where HDEMG and kinematic data were analyzed. For forward reaching, the electrode grid contralateral to the less affected/dominant arm was considered for analysis. For lateral reaching, the side where the participants could reach further was chosen for data analysis and the electrode grid contralateral to the reaching arm was analyzed. Our choice was based on previous studies showing greater activity in the contralateral ES during unilateral upper-limb movement (40, 41). To evaluate changes in the regional activity within the reaching movement, differences in the y-axis centroid values between the reaching and returning phases were calculated. We considered the influence of reaching distance on the ES activity as individuals with SCI likely reached a shorter distance than the control. Therefore, we additionally analyzed the part of the HDEMG data in the controls when they reached a similar distance to the participants with SCI.

Statistical Analysis

SPSS version 27 (IBM Corp., Armonk, NY) was used for statistical analysis. Data were tested for normality using the Shapiro–Wilk test. When the data distribution failed the normality test, nonparametric tests were applied. For the RSF and external perturbation tasks, independent t or Mann–Whitney U tests were used to compare HDEMG parameters (EMG amplitude; x-axis and y-axis of the centroid) and kinematic measurements (displacement of wrist, trunk, and CoP; total trajectory) during the APA and the CPA windows and velocity of the arm movement between individuals with SCI and the controls. For multidirectional reaching tasks, mixed-

Downloaded from journals.physiology.org/journal/jn at Imperial Col London (2A0C:5BC0:0040:1008:1A60:24FF:FEA6:CAE5) on July 16, 2025.

model repeated-measures ANOVAs with movement phase (reaching vs. returning) as repeated measures and group (controls vs. SCI) as the between-group variable were performed on the HDEMG data. When there was a main effect, a post hoc analysis was used. Independent t or Mann–Whitney U tests were applied for between-group (controls vs. SCI) comparisons on changes in y-axis centroid location and kinematic data during the reaching tasks. Correlation analyses were used to determine the relationship between APA and CPA phases, as well as to identify any relationships between the level of injury, the HDEMG-derived parameters, and kinematic data in participants with SCI. Significance of the results was set at $P \leq 0.05$. Data are presented as mean [standard deviation (SD)] or median (range) in the text. Effect sizes (η^2p) and 95% confidence intervals are reported.

RESULTS

Demographics

There was no difference in age between the SCI and the control groups ($t = -0.15$; $P = 0.89$). There were 10 more males in the SCI group (17 men) than in the control group [7 men; X^2 (1, $n = 42$) = 9.7, $P = 0.004$]. Of 21 participants with SCI, three were categorized as AIS B (14%), 10 were C (48%), and 8 were D (38%); 16 participants with SCI had cervical SCI (76%) and five had thoracic SCI (24%). Details of the demographic data of the participants with SCI are presented in Table 1.

Activation Onset of the ES during Rapid Shoulder Flexion

Figure 2*A* illustrates rectified EMG traces averaged across five repetitions of the RSF task from a control participant and an individual with an SCI at C3 (ID# 14 from Table 1).

Table 1. *Demographic characteristics of participants with SCI*

ID	Sex	Age, yr	AIS Score	Level of Injury	Time since Injury, Years
1	M	53	C	C5	4
2	F	71	D	C6	59
3	M	80	D	T4	7
4	M	59	C	C5	3
5	M	23	C	C4	4
6	M	47	C	C3	5
7	M	49	C	C3	4
8	M	52	C	T2	7
9	M	69	D	T7	10
10	M	69	D	C4	3
11	F	50	C	T2	2
12	M	52	D	C3	1
13	M	54	B	C5	19
14	M	63	D	C3	7
15	M	50	C	C4	1
16	F	52	D	C6	1
17	M	50	D	C4	15
18	M	53	B	C5	7
19	M	67	C	T10	5
20	F	36	B	C6	2
21	M	60	C	C3	2

AIS, American Spinal Injury Association Impairment Scale; F, female; M, male; SCI, spinal cord injury.

Note that the EMG onset of ES is earlier than the EMG onset of AD in the control, while the EMG onset of ES is after the EMG onset of AD in the individual with SCI. Given that EMG onset of AD and ES, and the HDEMG-derived parameters did not differ between sides, the values of left and right sides were averaged. HDEMG data from two participants with SCI were removed due to signal noise in many channels; one participant with SCI did not have valid AD EMG. Group results (Fig. 2, *B–D*) showed that participants with SCI ($n = 18$) had longer EMG onset of AD (median [range] 218.40 [381.85] ms; $Z = -3.14$; $P = 0.002$) and ES (228.70 [534.07] ms; $Z = -3.13$; $P = 0.002$), and delayed APAs (19.65 [125.80] ms; $Z = -3.62$; $P < 0.001$) during the RSF tasks, compared with the controls ($n = 21$; onset AD: 165.60 [168.25] ms; onset ES: 174.10 [177.38] ms; APAs: 3.60 [80.78] ms). In addition, the mean angular velocity of the arm movement was faster in the controls than in the participants with SCI (controls: 226.64 [39.55]°/s; SCI: 127.08 [78.80]°/s; $Z = 4.50$; $P < 0.001$).

Regional Activation of the ES during Rapid Shoulder Flexion

Figure 3*A* illustrates the spatial distribution of EMG amplitude of the ES in a representative control participant and an individual with SCI at C4 (ID# 17) during the RSF task. The upper panel represents the activation distribution during the APA window while the lower panel represents the activation distribution during the shoulder flexion window of the task (see the MATERIALS AND METHODS for details). Note that the spatial activation of the ES (i.e., y-axis of the centroid, white circle) is located more caudally in the individual with SCI than in the control. Group results demonstrated lower EMG amplitudes of the ES in participants with SCI (APA: median [range] 11.39 [36.46] μV; shoulder flexion: 10.62 [28.02] μV) than in the controls (APA: 22.34 [65.93] μV; shoulder flexion: 18.20 [27.95] μV) during both the APA ($Z = -2.88$, $P = 0.004$) and shoulder flexion ($Z = -3.21$; $P = 0.001$) windows (Fig. 3*B*). In addition, the y-axis of the centroid was located more caudally in the participants with SCI (APA: 6.80 [4.77] cm; shoulder flexion: 6.47 [5.12] cm) than in the controls (APA: 5.23 [4.33] cm; shoulder flexion: 4.15 [6.85] cm) in both the APA ($Z = -2.75$, $P = 0.006$) and the shoulder flexion ($Z = -3.51$, $P < 0.001$) windows (Fig. 3*B*), meaning that the activation of the ES during the RSF task was localized at the lower part of the grid in the individuals with SCI, while the activation was centered more in the upper part of the grid in the controls. Furthermore, no differences were found in the CoP displacement between participants with SCI and controls during the RSF task ($Z = -1.05$, $P = 0.293$; Table 2). There was no correlation between the level of injury and EMG amplitude, x-axis or y-axis of the centroid, or CoP displacement in the participants with SCI ($P > 0.05$ for all cases).

Regional Activation of the ES during the External Perturbation Task

HDEMG data from three participants with SCI and one control participant were excluded due to signal noise. No difference in activation onset of the ES with respect to the impact of the perturbation was found between individuals with SCI (median [range] −213.70 [271.50] ms; $n = 14$) and the controls (−157.70 [270] ms; $n = 20$) during the external

Downloaded from journals.physiology.org/journal/jn at Imperial Col London (2A0C:5BC0:0040:1008:1A60:24FF:FEA6:CAE5) on July 16, 2025.

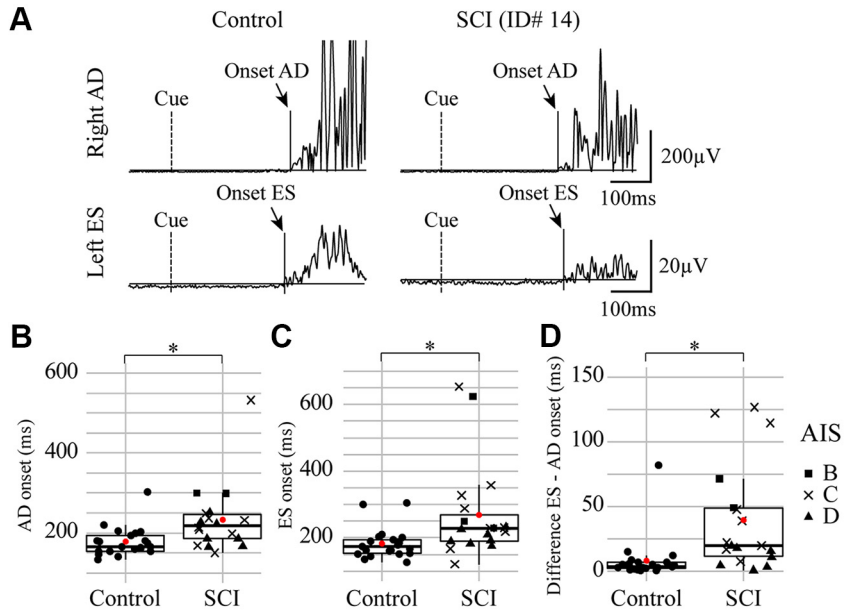


Figure 2. EMG onset during rapid shoulder flexion. *A*: raw EMG traces recorded from right anterior deltoid (AD) and left erector spinae (ES) from a control participant and an individual with C3 SCI (ID# 14 from Table 1) during the rapid shoulder flexion (RSF) task. The dashed vertical line represents the visual cue. The solid vertical line indicates the EMG onset. The black horizontal line is the level of the mean plus 3 SD. Note that the onset of ES is before that of AD in the control participant, while the onset of ES is later than that of AD in the individual with SCI. Onset results for AD (*B*), ES (*C*), and delayed APAs (*D*) for SCI ($n = 18$, males $n = 15$) and control ($n = 21$, males $n = 7$) groups. The horizontal line within the box represents the median, and outer edges of the box represent the 25th and 75th percentiles. The upper and lower whiskers extend to 1.5 times the interquartile range. The red dot indicates the mean value. *$P < 0.05$ between-group comparisons with Mann–Whitney *U* test. SCI, spinal cord injury.

perturbation task ($Z = -1.35$, $P = 0.18$). Figure 4*A* illustrates the spatial distribution of EMG amplitude of the ES during the APA (top) and CPA (bottom) phases of the external perturbation obtained from a control participant and an individual with an SCI at C3 (ID# 6). Note that the *y*-axis of the centroid of the EMG amplitude map (large white circle) is located at a more caudal region of the grid in the individual with SCI, whereas it is positioned more cranially in the control, during both APA and CPA phases. The group results (Fig. 4*B*) confirmed that the *y*-axis of the centroid was located more caudally in the individuals with SCI (APA: means [SD] 5.81 [1.90] cm; CPA: 6 [1.71] cm) than in the controls (APA: 4.56 [1.33] cm; CPA: 4.70 [1.38] cm) during both APAs [$t(36) = -2.37$, $P = 0.023$, 95% CI −2.32 to −0.18] and CPAs [$t(36) = -2.59$, $P = 0.014$, 95% CI −2.31 to −0.28]. However, the EMG amplitude was not different between the

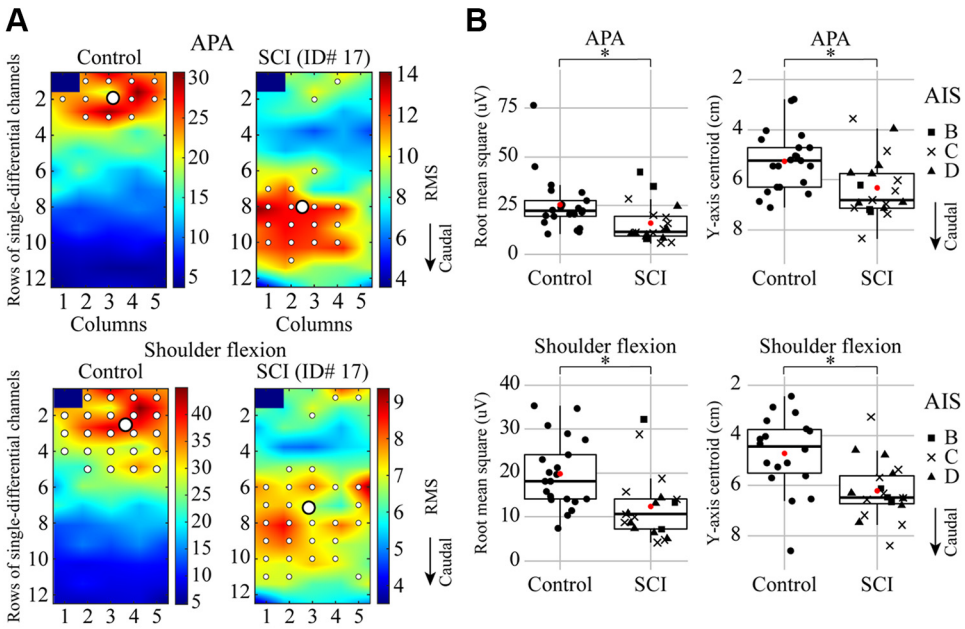


Figure 3. HDEMG in the rapid shoulder flexion (RSF) task. *A*: differential EMG amplitude maps of the ES based on two analysis windows: APA and the shoulder flexion phase of the task from a control participant and an individual with C4 SCI (ID# 17). Note that the *y*-axis of the centroid location (large white circle) is located at the center or lower part of the grid in the individual with SCI, while that is located at the upper part of the grid in the control. The smaller circles represent the active channels, meaning those with an RMS amplitude higher than 70% of the maximum RMS amplitude across the grid. *B*: group data of EMG amplitude and *y*-axis of the centroid of the ES (controls $n = 21$, males $n = 7$; SCI $n = 19$, males $n = 16$). The horizontal line within the box represents the median, and outer edges of the box represent the 25th and 75th percentiles. The upper and lower whiskers extend to 1.5 times the interquartile range. The red dot indicates the mean value. *$P < 0.05$ between-group comparisons with Mann–Whitney *U* test. APA, anticipatory postural adjustment; RMS, root mean square; SCI, spinal cord injury.

Downloaded from journals.physiology.org/journal/jn at Imperial Col London (2A0C:5BC0:0040:1008:1A60:24FF:FEA6:CAE5) on July 16, 2025.

Table 2. *Kinematic results in control participants and individuals with SCI*

Task	Measurements, mm	Mean/Median, SD/range	Statistics
Rapid shoulder flexion task	CoP displacement A-P	C: 30.06 (63.88) SCI: 23.05 (40.55)	$Z = -1.05$, $P = 0.293$
	CoP total trajectory	C: 183.68 (166.35) SCI: 210.03 (192.14)	$Z = -1.50$, $P = 0.135$
External perturbation task	APA - CoP displacement A-P	C: 2.06 (6.61) SCI: 2.49 (12.42)	$Z = -0.14$, $P = 0.89$
	APA - CoP total trajectory	C: 10.00 (2.24) SCI: 9.23 (3.13)	$t(37) = 0.89$, $P = 0.381$, 95% CI −0.99 to 2.53
	CPA - CoP displacement A-P	C: 6.18 (16.86) SCI: 5.88 (11.02)	$Z = -0.31$, $P = 0.76$
	CPA - CoP total trajectory	C: 11.51 (12.31) SCI: 13.19 (12.28)	$Z = -0.45$, $P = 0.65$
Forward reaching	Wrist displacement A-P	C: 488.13 (89.50) SCI: 244.11 (117.21)	$t(39) = 7.52$, $P < 0.001$*, 95% CI 178.34–309.70
	T1 displacement A-P	C: 514.34 (351.17) SCI: 287.83 (416.93)	$Z = -4.98$, $P < 0.001$*
	CoP displacement A-P	C: 138.38 (110.60) SCI: 62.46 (129.76)	$Z = -4.97$, $P < 0.001$*
	CoP total trajectory	C: 327.83 (234.53) SCI: 209.78 (288.38)	$Z = -5.03$, $P < 0.001$*
Lateral reaching	Wrist displacement M-L	C: 275.55 (221.62) SCI: 93.17 (242.18)	$Z = -4.10$, $P < 0.001$*
	T1 displacement M-L	C: 284.24 (65.72) SCI: 147.14 (87.15)	$t(39) = 5.71$, $P < 0.001$*, 95% CI 88.49–185.70
	CoP displacement M-L	C: 140.96 (33.73) SCI: 69.45 (35.90)	$t(36) = 6.33$, $P < 0.001$*, 95% CI 48.60–94.42
	CoP total trajectory	C: 355.78 (78.92) SCI: 287.82 (91.77)	$t(36) = 2.45$, $P = 0.019$*, 95% CI 11.80–124.12

A-P, anterior-posterior; APA, anticipatory postural adjustment; C, controls; CoP, center of pressure; CPA, compensatory postural adjustment; M-L, medio-lateral; SCI, spinal cord injury; T1, 1st thoracic spinous process; *$P < 0.05$ between-group comparisons with Mann–Whitney U test (Z value; median, range reported) or independent t test (t value; means, SD reported).

groups during the APA (SCI: median [range] 6.90 [41.06] μV; Control: 7.69 [12.34] μV) and CPA (SCI: 9.99 [45.41] μV; Control: 9.71 [21] μV) phases ($P > 0.05$ for both; Fig. 4*B*). No differences were found in the CoP displacement during APA or CPA phases between the SCI ($n = 19$) and control ($n = 20$) groups ($P > 0.05$ for both; Table 2). No correlations were found between the level of injury, HDEMG-derived parameters, or CoP displacement in individuals with SCI ($P > 0.05$ for all cases).

Regional Distribution of ES Activity during Multidirectional Reaching Tasks

One participant with SCI was unable to perform the reaching tasks; HDEMG data from three participants with SCI were excluded due to movement artifacts. As expected, individuals with SCI reached with shorter distance and had smaller trunk and CoP displacement in both forward and lateral reaching compared with the controls (Table 2). Figure 5*A*

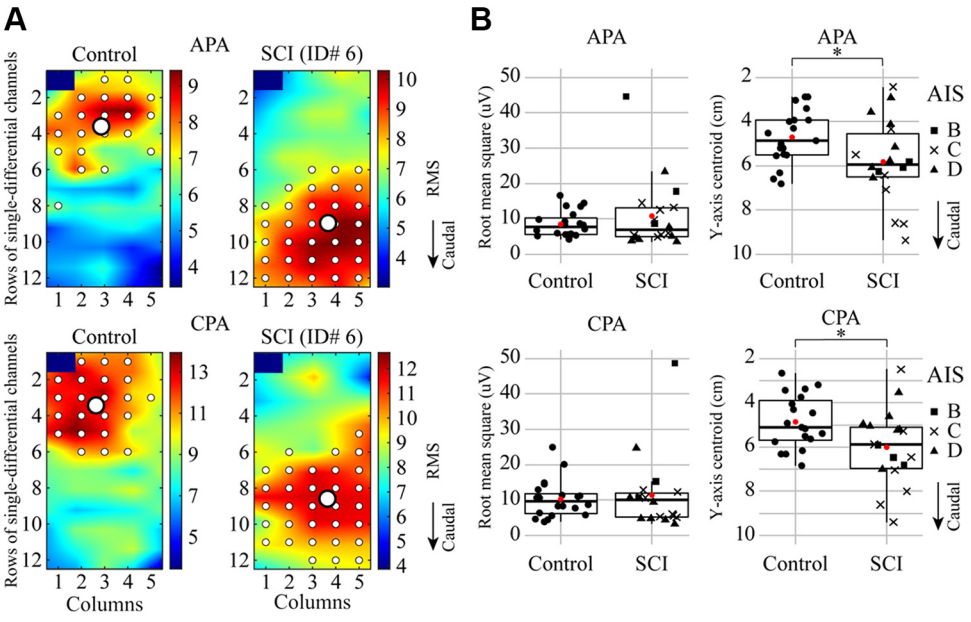


Figure 4. HDEMG of the external perturbation task. *A*: differential EMG amplitude maps of the ES in the APA (−100 ms to 50 ms; *top*) and CPA (50 ms to 200 ms; *bottom*) windows obtained from a control participant and an individual with C3 SCI (ID# 6). The large white circle represents the *y*-axis centroid, whereas the smaller white circles represent the active channels, meaning those with an RMS amplitude higher than 70% of the maximum RMS amplitude across the grid. *B*: group data of EMG amplitude and *y*-axis of the centroid of the ES (controls $n = 20$, males $n = 7$; SCI $n = 18$, males $n = 15$). The horizontal line within the box represents the median, and outer edges of the box represent the 25th and 75th percentiles. The upper and lower whiskers extend to 1.5 times the interquartile range. The red dot indicates the mean value. *$P < 0.05$ between-group comparisons with independent t test. APA, anticipatory postural adjustment; CPA, compensatory postural adjustment; SCI, spinal cord injury.

Downloaded from journals.physiology.org/journal/jn at Imperial Col London (2A0C:5BC0:0040:1008:1A60:24FF:FEA6:CAE5) on July 16, 2025.

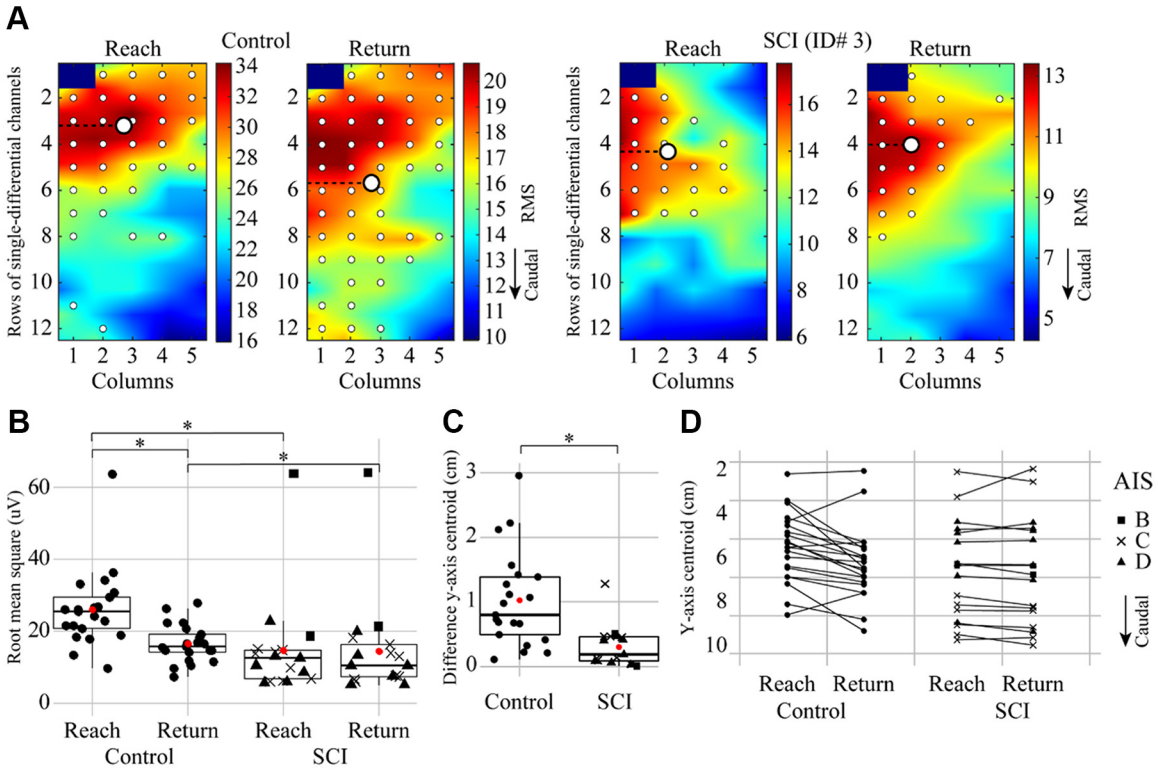


Figure 5. HDEMG during forward reaching. *A*: differential EMG amplitude maps of the ES based on the reaching (*left*) and returning (*right*) phases of the task obtained from a control participant and an individual with T4 SCI (ID# 3). Note that activation of the ES is limited in an area in the individual with SCI, while the activation is more spread out in the control. The large white circle represents the *y*-axis centroid, whereas the smaller white circles represent the active channels, meaning those with an RMS amplitude higher than 70% of the maximum RMS amplitude across the grid. *B*: group data of EMG amplitude (controls $n = 21$, males $n = 7$; SCI $n = 17$, males $n = 14$). The horizontal line within the box represents the median, and outer edges of the box represent the 25th and 75th percentiles. The upper and lower whiskers extend to 1.5 times the interquartile range. The red dot indicates the mean value. *C*: group data of the difference in the *y*-axis of the centroid (controls $n = 21$, males $n = 7$; SCI $n = 17$, males $n = 14$) between the reaching and returning phases. *D*: individual differences in the *y*-axis of the centroid between reaching and returning phases. *$P < 0.05$ with repeated-measures ANOVA and post hoc tests. RMS, root mean square; SCI, spinal cord injury.

illustrates the spatial distribution of EMG amplitudes of the ES during forward reaching obtained from a control participant and an individual with an SCI at T4 (ID# 3). Note that the *y*-axis centroid changes during reaching and returning phases in the control, while it remains at the same location in the participant with SCI. A repeated-measures ANOVA demonstrated a large effect of movement phase ($F_{1,36} = 30.03$, $P < 0.001$; $\eta^2p = 0.46$), and an interaction of movement phase × group ($F_{1,36} = 28.63$, $P < 0.001$; $\eta^2p = 0.44$) on EMG amplitude during forward reaching (SCI = 17, control = 21). Post hoc analyses revealed greater EMG amplitude during the reaching phase (median [range] 25.56 [54.05] μV) than the returning phase (15.61 [20.65] μV) in the controls ($Z = -4.02$, $P < 0.001$), whereas the EMG amplitude was not different between the two phases of the reaching movement in the participants with SCI (Reach: 12.45 [58.36] μV; Return: 10.39 [59.06] μV; $Z = -0.40$, $P = 0.687$; Fig. 5*B*). In addition, EMG amplitude was lower in individuals with SCI than in the controls during the reaching phase ($Z = -3.95$, $P < 0.001$; Fig. 5*B*) and during the returning phase ($Z = -2.22$, $P = 0.027$; Fig. 5*B*) of the task. For the *y*-axis of the centroid, there was a small-to-medium effect of movement phase ($F_{1,36} = 10.14$, $P = 0.003$; $\eta^2p = 0.22$) and an interaction of movement phase × group ($F_{1,36} = 6.81$, $P = 0.013$; $\eta^2p = 0.16$) during forward reaching. When comparing the changes in the *y*-axis of the centroid from reaching to returning phases between participants with SCI and the controls, the difference was greater in the controls (median [range] 0.79 [2.85] cm) than in the participants with SCI (0.19 [1.27] cm; $Z = -3.74$; $P < 0.001$; Fig. 5, *C* and *D*). No significant correlations were found between the level of injury and RMS amplitude, *x*-axis or *y*-axis of the centroid, reaching distance, or the CoP displacement in the participants with SCI ($P > 0.05$ for all cases).

Figure 6*A* illustrates the spatial distribution of EMG amplitudes of the ES during lateral reaching in a control participant and an individual with T4 SCI (ID# 3), showing distinct spatial activation patterns between the individual with SCI and the control. The results revealed a significant effect of movement phase ($F_{1,37} = 8.68$, $P = 0.006$; $\eta^2p = 0.19$) and an interaction of movement phase × group ($F_{1,37} = 21.52$, $P < 0.001$; $\eta^2p = 0.37$) with a medium-to-large effect size on EMG amplitude during lateral reaching (SCI = 18, control = 21). Post hoc analyses showed that EMG amplitude was greater during the reaching phase (median [range] 15.22 [34.30] μV) than during the returning phase (12.21 [23.56] μV) in the controls ($Z = -3.67$, $P < 0.001$; Fig. 6*B*). In the SCI group, EMG amplitude was lower during the reaching phase (11.40 [35.69] μV) than during the returning phase (11.92 [36.07] μV), albeit the difference was small ($Z = -2.16$, $P = 0.031$; Fig. 6*B*). In addition, EMG amplitude of the ES was

Downloaded from journals.physiology.org/journal/jn at Imperial Col London (2A0C:5BC0:0040:1008:1A60:24FF:FEA6:CAE5) on July 16, 2025.

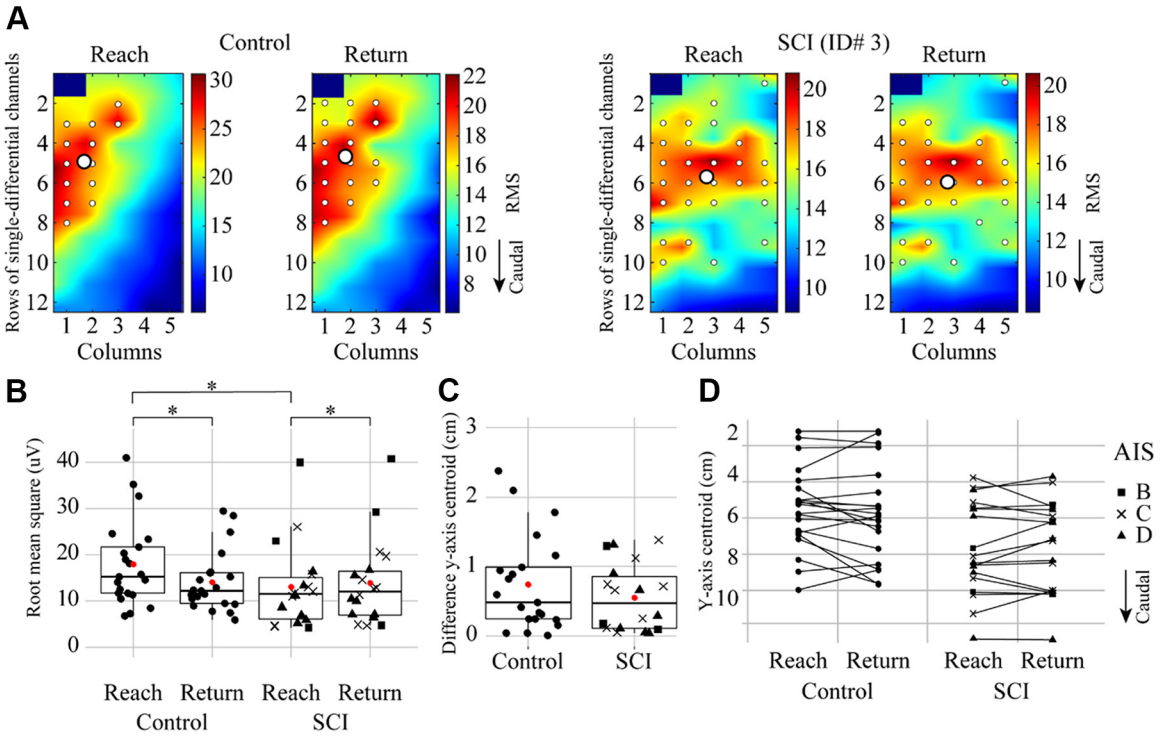


Figure 6. HDEMG of lateral reaching. *A*: differential EMG amplitude maps of the ES based on the reaching (*left*) and returning (*right*) phases of the movement obtained from a control participant and an individual with T4 SCI (ID# 3). Note that activation is located more caudally in the individual with SCI in contrast to the control. The large white circle represents the *y*-axis centroid, whereas the smaller white circles represent the active channels, meaning those with an RMS amplitude higher than 70% of the maximum RMS amplitude across the grid. *B*: group results of EMG amplitude (controls $n = 21$, males $n = 7$; SCI $n = 18$ males $n = 15$). The horizontal line within the box represents the median, and outer edges of the box represent the 25th and 75th percentiles. The upper and lower whiskers extend to 1.5 times the interquartile range. The red dot indicates the mean value. *C*: group data of the difference in the *y*-axis of the centroid (controls $n = 21$, males $n = 7$; SCI $n = 18$, males $n = 15$) between the reaching and returning phases. *D*: individual differences of the *y*-axis of the centroid between reaching and returning phases. *$P < 0.05$ with repeated-measures ANOVA and post hoc tests. RMS, root mean square; SCI, spinal cord injury.

greater in the controls than in the participants with SCI during the reaching phase ($Z = -2.00$, $P = 0.045$) but not during the returning phase ($Z = -0.59$, $P = 0.554$; Fig. 6*B*). For the *y*-axis of the centroid, there was no effect of movement phase ($F_{1,37} = 0.42$, $P = 0.521$; $\eta^2p = 0.01$) or an interaction of movement phase × group ($F_{1,37} = 1.73$, $P = 0.196$; $\eta^2p = 0.05$) in the lateral reaching. There was no between-group difference (Control: median [range] 0.48 [2.37] cm; SCI: 0.47 [1.34] cm) in the change in the *y*-axis of the centroid between the reaching and returning phases ($Z = -0.79$; $P = 0.43$; Fig. 6, *C* and *D*). No correlations were found between the level of injury and EMG amplitude, *x*-axis or *y*-axis of the centroid, reaching distance, or the CoP displacement ($P > 0.05$ for all cases).

We performed additional analyses on the HDEMG data when the reaching distance of the controls was matched to the participants with SCI. All results remained the same as the main results described earlier (Supplemental Figs. S1 and S2; all Supplemental material is available at https://doi.org/10.5281/zenodo.8394954).

DISCUSSION

The current study aimed to characterize the spatial distribution of activation from the thoracic part of the ES in individuals with an incomplete SCI during postural tasks and multidirectional reaching tasks. Our findings demonstrate a more caudally distributed activation of the ES during the postural tasks in individuals with SCI, compared with the controls. In addition, phase-dependent activation of the ES was lost during the reaching tasks in individuals with SCI. Specifically, the *y*-axis of the centroid did not change during forward reaching in the individuals with SCI. The EMG amplitude of ES was the same between reaching forward and returning to the upright posture in individuals with SCI, while the EMG amplitude was greater in reaching forward compared with returning to the upright posture in the controls, suggesting a loss of discrete control of the ES after SCI. These differences in regional distribution in ES were still present even when the kinematic results were matched between the groups. We suggest that altered regional activation of the thoracic ES seen in postural adjustments and movements of the trunk may reflect compensatory trunk control strategies using residual muscle fibers of the ES for functional reservation after SCI.

Altered Regional Distribution of ES Activity for Postural Control after SCI

The cranio-caudal shift of activation of the ES observed in our study may be related to the innervation zones of the ES predominantly distributed in a narrow band along the muscle fibers in the superior-inferior direction (25, 26). Studies investigating regional distribution of activation of

Downloaded from journals.physiology.org/journal/jn at Imperial Col London (2A0C:5BC0:0040:1008:1A60:24FF:FEA6:CAE5) on July 16, 2025.

biceps brachii and tibialis anterior reported a shift in activation along the direction of the muscle fibers when the contraction levels (42) and walking speed (43), respectively, were increased. Here, we observed delayed activation of the ES with respect to the AD (i.e., delayed APAs) during the RSF task in individuals with SCI, with the activation being lower and more caudally distributed, compared with the controls. Our results support previous work showing delayed APAs in people with SCI (7). APA is a feedforward control mechanism and is thought to be mediated by the motor cortex as it occurs in a time window (−100 to +50 ms with respect to initiation of a movement) (44) either before a movement or too early to be influenced by afferent input from the periphery (44–46). Previous studies reported an association between corticospinal excitability and timing of APAs in adults with SCI (7) and in older adults (47), suggesting a relationship between corticospinal function and postural control. As the corticospinal function is impaired after SCI, we suggest that the change in regional distribution of ES activity may be resulted from impaired synaptic connections between descending motor pathways and motor neurons in the spinal cord. Furthermore, prior work suggests that the APA response was influenced by limb movement velocity only when the movement was below a threshold velocity, i.e., 100°/s (35). Although the mean velocity of the arm movement was slower in participants with SCI than in the controls, it was above 100°/s in the participants with SCI, exceeding the velocity threshold for the involvement of APAs. Nevertheless, caution is needed when interpreting the ES activation and APAs induced by the RSF task.

Similar results were found during the external predicted perturbation task. Individuals with SCI activated the caudal part of the ES while the controls recruited the cranial part of the ES in both APA and CPA windows. Different from APA, CPA is a feedback control mechanism involving sensorimotor integration (48). Thus, different regional distribution of ES activity during the external predicted perturbation task may be due to impaired sensorimotor function after SCI.

An intriguing question is why was the activation of the ES at the lower level of the thoracic ES (closer to lumbar ES) in individuals with incomplete SCI? Prior work reported that people with SCI often adopt a posterior pelvic tilt that flexes the thoraco-lumbar spine to increase the base of support and improve trunk stability and sitting balance (49, 50). It is possible that this compensatory postural control strategy influenced the regional distribution of ES activity, thus a more caudally distributed activation, in individuals with SCI. However, when we matched the sitting posture of the control participants to the participants with SCI, i.e., the control participants were seated with a posterior pelvic tilt and performed the tasks, their ES activation did not shift to the lower part of the ES, as seen in participants with SCI (Supplemental Figs. S3 and S4). Prior work reported similar thoracic ES activity between upright sitting and slouched sitting in healthy adults (51), suggesting a limited influence of posture on thoracic ES activity. Nevertheless, while we did not observe acute changes in ES activation with alterations in sitting posture, as demonstrated in control participants, this may not fully capture the chronic changes in the ES activation associated with sitting posture in individuals with SCI. Another possible explanation could be altered synaptic connections between the descending motor axons and motor neurons after SCI. Animal studies have demonstrated sprouting of the descending axons innervating spinal motoneurons caudal to the lesion site (52, 53). For instance, an injury in the thoracic spinal cord of rats led to the descending axonal sprouts, which subsequently formed new synaptic connections with propriospinal neurons projecting to lumbar motor neurons (53). Research in humans with incomplete SCI reported increased corticospinal excitability of muscles distant from the point of injury, while the excitability remained unchanged in muscles at and above the injury level (54), suggesting the caudal synaptic connections from an injury to maintain a supraspinal influence to distal spinal segments after SCI. Taken together, the results presented in this study revealed the differential activation of specific regions of the ES for postural control after SCI. We suggest that the caudal shift in ES activation could reflect reinnervation and alterations in the selective neural control of the ES to allow for activating the residual muscle fibers that are advantageous for postural control and movement after SCI. The extent to which changes in ES activation underpin task performance warrants further investigation.

Altered Spatial Distribution of the ES Activity for Assisting with Movements of the Upper Extremities after SCI

Research using indwelling EMG electrodes has shown distinct muscle activation between the caudal and cranial regions of the lumbar ES during goal-directed voluntary movement of the trunk in noninjured adults, suggesting selective control of regions of the ES (11). During forward and lateral reaching, the ES was activated for the trunk moving closer to the target and then returning to the original posture, thereby a goal-directed movement of the trunk. Here, we observed greater ES activity during the reaching phase than the returning phase in the controls, while the ES activity between the two phases was not different in individuals with SCI. Our results support previous studies showing that individuals with SCI used more co-contractions and less directional tuning of the trunk muscles when leaning the body toward multiple directions, compared with the noninjured adults (15, 55). Increased co-contraction of muscles during motor tasks has been shown in animals and humans with SCI (56–58), likely due to reduced supraspinal influence and greater motoneuron excitability (58, 59). Use of co-contraction of the trunk muscles during functional reaching may reflect an altered trunk control strategy to stiffen the trunk (60). Our study reveals the altered trunk control strategy spatially and future investigations on quantifying spatial activation across different trunk muscles for evaluation of the trunk motor strategy after SCI are needed. Moreover, the activity of the ES was limited to a smaller region of the ES within the forward-reaching movement in participants with SCI, while it was spread across the muscle in the controls. We did not observe differences in the *y*-axis centroid between the controls and participants with SCI during lateral reaching. However, previous studies using surface HDEMG have consistently showed differences in the centroid position along the direction of the muscle fibers (i.e., *y*-axis

Downloaded from journals.physiology.org/journal/jn at Imperial Col London (2A0C:5BC0:0040:1008:1A60:24FF:FEA6:CAE5) on July 16, 2025.

centroid for the ES) but little variation across the fibers (i.e., *x*-axis centroid) (32, 61). Movement of the lateral reaches occurs on the frontal plane and any changes in the regional activation are more likely to be observed on the *x*-axis centroid (lateral-medial of the ES), which may explain the lack of changes in the centroid position during lateral reaching. When comparing the ES activity for a similar reaching distance between the groups (i.e., we analyzed a portion of the data of reaching in the controls), the differences in the SCI group remained (Supplemental Figs. S1 and S2). It is thought that changes in EMG amplitude within the muscle reflect task- or movement-specific motor control, possibly due to selective control from the central nervous systems (62–64). A localized activation of the ES in those with SCI may be related to impairment of selective neural control of the ES and hence altered motor control strategies of the trunk. It should be noted that a shift in the regional activation toward the caudal region of the thoracic ES could be a result of a nonspecific (generalized) activation over the entire electrode grid that may be more related to muscle weakness of the ES after SCI. Nevertheless, this possibility was controlled by our analysis approach that only considered the electrodes with an RMS amplitude higher than 70% of the maximum RMS amplitude of the entire electrode grid. Given the small activity obtained in the impaired trunk muscles in individuals with SCI, this approach improved the signal-to-noise ratio, allowing for better detection of differences in the activation pattern of the ES between individuals with SCI and the controls. Furthermore, the differences in regional activation could also be influenced by the architecture of the muscle (e.g., direction of the muscle fibers, innervation zone) and changes in the interelectrode distance during the movement (e.g., movement of the skin) (65). The latter one is less likely as regional distribution of ES activity remained to be different between SCI and control participants when the reaching distance was matched. Therefore, the distinct distribution of the EMG response in the ES between our participants with chronic SCI and the controls in our study could be due to a combination of impaired synaptic input to the muscles below the injury (7, 54, 66) and changes in the properties of the ES muscles, such as muscle atrophy (67, 68), denervation (69), and changes in signaling transmissions around the neuromuscular junctions (70), that have been reported to occur following SCI.

Furthermore, it is possible that some participants with SCI used their nonreaching arm for stability during functional reach tasks, despite care being given during the data collection and trials, which did not comply with the instructions being discarded. Prior work recorded EMG from bilateral ES during unilateral shoulder abduction with the right arm in healthy adults (41). They reported no change in EMG activity of the right (ipsilateral) ES when increasing contraction levels of the arm. The same phenomenon was observed in this study in both participants with SCI and controls. Although we cannot fully exclude the influence of the use of the nonreaching arm on the results of EMG, our results are in keeping with previous studies that reported different EMG amplitudes of the trunk muscles between individuals with SCI and controls during reaching (5, 15). Moreover, some of the participants included in this study (i.e., AIS B) had more severe injuries than others. Those participants could have different EMG results from the other participants due to severe impairment of motor function below the level of injury. However, the small sample size precluded a subgroup analysis in this study.

Functional Consequences

Surface bipolar EMG has been extensively used to study trunk muscle control, and muscle synergies of upper body and back muscles in individuals with chronic SCI (7, 15, 71–74). Emerging evidence has shown the CNS selectively controlling different regions of the ES and the nonuniformity of activation of the ES across spinal segments during trunk movements in noninjured adults (11, 75, 76). Hence, it is important to assess injury-related changes in the spatial activation of the ES muscles to gain insight into the use of residual muscle fibers of the ES for function after SCI. HDEMG can provide detailed information on activation patterns of the ES that bipolar EMG is unable to provide. Indeed, we show that individuals with SCI recruited a different part of the thoracic ES during tasks requiring postural stability and involving movements of the upper extremities. Our results echo previous studies showing changes in trunk muscle activity during functional activities, such as in wheelchair propulsion (77, 78) and during pivot transfers (79), after SCI. In addition, our findings provide spatial changes in neuromuscular control of the trunk across spinal segments below the level of injury in individuals with incomplete SCI.

Prior work using machine learning approaches was able to classify different motor tasks based on the spatial-temporal information extracted from HDEMG in people with incomplete SCI (80), with a view to developing assistive technologies for upper limb function. Research has also shown improved diagnosis of paralysis of hand muscles in individuals with SCI using HDEMG with advanced signal processing techniques (81). Furthermore, surface EMG is common in clinical research settings for evaluation of therapeutic outcomes of trunk rehabilitation (82, 83). Given that trunk control plays an important role in activities of daily living and many people living with SCI have impaired trunk control, our findings provide new insight into motor control of the ES in SCI, relevant to development of assistive technology for postural control, assessment of trunk muscles, and evaluation of therapies for trunk function.

Limitations

There are limitations in this study. First, results were presented without EMG normalization, as our previous study reported that with the same technique and the methodology uncorrected EMG amplitudes seem to be more reliable than normalized data (27). People with SCI tend to have a higher body mass index that can influence the magnitude of EMG signals. We did not observe consistent lower EMG amplitudes across the tasks in the participants with SCI. In addition, our results focused on regional distribution of ES activity that is less affected by the between-subject differences in magnitude of EMG signals. Another limitation was that there were fewer male participants in the control group than in the SCI group. More male participants in the SCI group are in keeping with the prevalence of SCI being higher in males than in females (84). The effect of sex on EMG

Downloaded from journals.physiology.org/journal/jn at Imperial Col London (2A0C:5BC0:0040:1008:1A60:24FF:FEA6:CAE5) on July 16, 2025.

measurements has been reported during high levels of sustained voluntary contractions (85–88). Nevertheless, prior work reported no sex differences in muscle activity during intermittent low levels of voluntary contractions (89) and our unpublished work did not detect sex differences in the HDEMG-derived parameters in the ES during the reaching tasks. Although we are unable to completely rule out the effect of sex in our results, the impact of the imbalance of male and female participants between the groups on our results is likely to be minimal. Moreover, as there were only five participants with a thoracic SCI, we did not perform a subgroup analysis comparing spatial activation of the ES between participants with high-thoracic and low-thoracic SCI. A relatively small sample size in our study may contribute to the absence of significant correlations between the level of injury and HDEMG-derived parameters. Previous studies using bipolar EMG reported different activity of the trunk muscles between individuals with high and low level of complete and incomplete SCI during static sitting (15, 72) and posterior transfer, which involves lifting the body up and shifting the body weight backward with bilateral upper extremities (90), albeit the information from the amplitude-based analysis with the bipolar EMG may not be applicable to the spatial activation of the muscles extracted from HDEMG. Finally, the interelectrode distance could change more in the controls than in the participants with SCI during reaching because the controls moved the trunk further than the participants with SCI. However, the influence is likely to be minimum as we did not observe similar centroid position when comparing the ES activity for a similar reaching distance between the groups (Supplemental Figs. S1 and S2).

Conclusions

We show that individuals with chronic, incomplete SCI recruited different regions of the thoracic ES to maintain postural stability and to move the trunk in assisting movements of the upper extremities. Specifically, the activation was shifted toward the caudal region of the ES and the discrete control of the ES was lost in individuals with SCI. We propose that these injury-related changes in the spatial activation of the ES are likely to represent the utilization of residual muscle fibers and alterations in selective neural control of the ES to maximize the ability to maintain posture and function.

DATA AVAILABILITY

The datasets generated and/or analyzed during the current study are not publicly available because patient data need to be handled in accordance with the current data protection laws and ethical guidelines but are available from the corresponding author on reasonable request.

SUPPLEMENTAL MATERIAL

Supplemental Figs. S1–S4: https://doi.org/10.5281/zenodo.8394954

ACKNOWLEDGMENTS

We thank all the participants for their participation and Mr. Ignacio Contreras Hernández for assistance during data collection.

GRANTS

The INSPIRE Foundation funded the study (to S.-Y. Chiou, P.H. Strutton, E. Martinez-Valdes, D.Falla, J.R. Chowdhury; funder grant reference: Trunk Function).

DISCLAIMERS

The funders had no influence on the design of the study, analysis, interpretation of the data, or in writing the manuscript.

DISCLOSURES

No conflicts of interest, financial or otherwise, are declared by the authors.

AUTHOR CONTRIBUTIONS

P.H.S., E.M.-V., D.F., J.R.C., and S.-Y.C. conceived and designed research; J.F.L.v.H., E.A., and S.-Y.C. performed experiments; J.F.L.v.H., H.V.C., E.A., and S.-Y.C. analyzed data; J.F.L.v.H., H.V.C., P.H.S., and S.-Y.C. interpreted results of experiments; J.F.L.v.H. and S.-Y.C. prepared figures; J.F.L.v.H. and S.-Y.C. drafted manuscript; J.F.L.v.H., H.V.C., P.H.S., E.M.-V., D.F., and S.-Y.C. edited and revised manuscript; J.F.L.v.H., H.V.C., E.A., P.H.S., E.M.-V., D.F., J.R.C., and S.-Y.C. approved final version of manuscript.

REFERENCES

1. **Farina D**, **Negro F**, **Dideriksen JL.** The effective neural drive to muscles is the common synaptic input to motor neurons. *J Physiol* 592: 3427–3441, 2014. doi:10.1113/jphysiol.2014.273581.
2. **Porter R**, **Lemon R.** *Corticospinal Function and Voluntary Movement*. Oxford: Oxford University Press, 1993.
3. **Lemon RN.** Descending pathways in motor control. *Annu Rev Neurosci* 31: 195–218, 2008. doi:10.1146/annurev.neuro.31.060407.125547.
4. **Oudega M**, **Perez MA.** Corticospinal reorganization after spinal cord injury. *J Physiol* 590: 3647–3663, 2012. doi:10.1113/jphysiol.2012.233189.
5. **Potten YJ**, **Seelen HA**, **Drukker J**, **Reulen JP**, **Drost MR.** Postural muscle responses in the spinal cord injured persons during forward reaching. *Ergonomics* 42: 1200–1215, 1999. doi:10.1080/001401399185081.
6. **Seelen HA**, **Potten YJ**, **Drukker J**, **Reulen JP**, **Pons C.** Development of new muscle synergies in postural control in spinal cord injured subjects. *J Electromyogr Kinesiol* 8: 23–34, 1998. doi:10.1016/s1050-6411(97)00002-3.
7. **Chiou SY**, **Strutton PH.** Crossed corticospinal facilitation between arm and trunk muscles correlates with trunk control after spinal cord injury. *Front Hum Neurosci* 14: 583579, 2020. doi:10.3389/fnhum.2020.583579.
8. **Milosevic M**, **Masani K**, **Kuipers MJ**, **Rahouni H**, **Verrier MC**, **McConville KM**, **Popovic MR.** Trunk control impairment is responsible for postural instability during quiet sitting in individuals with cervical spinal cord injury. *Clin Biomech (Bristol)* 30: 507–512, 2015. doi:10.1016/j.clinbiomech.2015.03.002.
9. **Bergmark A.** Stability of the lumbar spine. A study in mechanical engineering. *Acta Orthop Scand Suppl* 230: 1–54, 1989. doi:10.3109/17453678909154177.
10. **Moseley GL**, **Hodges PW**, **Gandevia SC.** Deep and superficial fibers of the lumbar multifidus muscle are differentially active during voluntary arm movements. *Spine (Phila Pa 1976)* 27: E29–E36, 2002. doi:10.1097/00007632-200201150-00013.
11. **Abboud J**, **Kuo C**, **Descarreaux M**, **Blouin JS.** Regional activation in the human longissimus thoracis pars lumborum muscle. *J Physiol* 598: 347–359, 2020. doi:10.1113/JP278260.
12. **Serafino F**, **Trucco M**, **Occhionero A**, **Cerone GL**, **Chiarotto A**, **Vieira T**, **Gallina A.** Understanding regional activation of thoracolumbar muscles in chronic low back pain and its relationship to clinically relevant domains. *BMC Musculoskelet Disord* 22: 432, 2021. doi:10.1186/s12891-021-04287-5.

Downloaded from journals.physiology.org/journal/jn at Imperial Col London (2A0C:5BC0:0040:1008:1A60:24FF:FEA6:CAE5) on July 16, 2025.

13. **Dimitrijevic MR**, **Dimitrijevic MM**, **Faganel J**, **Sherwood AM.** Suprasegmentally induced motor unit activity in paralyzed muscles of patients with established spinal cord injury. *Ann Neurol* 16: 216–221, 1984. doi:10.1002/ana.410160208.
14. **Galea MP.** Spinal cord injury and physical activity: preservation of the body. *Spinal Cord* 50: 344–351, 2012. doi:10.1038/sc.2011.149.
15. **Milosevic M**, **Yokoyama H**, **Grangeon M**, **Masani K**, **Popovic MR**, **Nakazawa K**, **Gagnon DH.** Muscle synergies reveal impaired trunk muscle coordination strategies in individuals with thoracic spinal cord injury. *J Electromyogr Kinesiol* 36: 40–48, 2017. doi:10.1016/j.jelekin.2017.06.007.
16. **Kouwijzer I**, **van der Meer M**, **Janssen TWJ.** Effects of trunk muscle activation on trunk stability, arm power, blood pressure and performance in wheelchair rugby players with a spinal cord injury. *J Spinal Cord Med* 45: 605–613, 2022. doi:10.1080/10790268.2020.1830249.
17. **Noamani A**, **Lemay JF**, **Musselman KE**, **Rouhani H.** Postural control strategy after incomplete spinal cord injury: effect of sensory inputs on trunk-leg movement coordination. *J Neuroeng Rehabil* 17: 141, 2020. doi:10.1186/s12984-020-00775-2.
18. **Chikh S**, **Garnier C**, **Faupin A**, **Pinti A**, **Boudet S**, **Azaiez F**, **Watelain E.** Arm-trunk coordination in wheelchair initiation displacement: a study of anticipatory and compensatory postural adjustments during different speeds and directions of propulsion. *J Electromyogr Kinesiol* 40: 16–22, 2018. doi:10.1016/j.jelekin.2018.03.001.
19. **Falla D**, **Gallina A.** New insights into pain-related changes in muscle activation revealed by high-density surface electromyography. *J Electromyogr Kinesiol* 52: 102422, 2020. doi:10.1016/j.jelekin.2020.102422.
20. **Gallina A**, **Merletti R**, **Gazzoni M.** Uneven spatial distribution of surface EMG: what does it mean? *Eur J Appl Physiol* 113: 887–894, 2013. doi:10.1007/s00421-012-2498-2.
21. **Gallina A**, **Disselhorst-Klug C**, **Farina D**, **Merletti R**, **Besomi M**, **Holobar A**, **Enoka RM**, **Hug F**, **Falla D**, **Sogaard K**, **McGill K**, **Clancy EA**, **Carson RG**, **van Dieen JH**, **Gandevia S**, **Lowery M**, **Besier T**, **Kiernan MC**, **Rothwell JC**, **Tucker K**, **Hodges PW.** Consensus for experimental design in electromyography (CEDE) project: high-density surface electromyography matrix. *J Electromyogr Kinesiol* 64: 102656, 2022. doi:10.1016/j.jelekin.2022.102656.
22. **Arvanitidis M**, **Jimenez-Grande D**, **Haouidji-Javaux N**, **Falla D**, **Martinez-Valdes E.** People with chronic low back pain display spatial alterations in high-density surface EMG-torque oscillations. *Sci Rep* 12: 15178, 2022. doi:10.1038/s41598-022-19516-7.
23. **Falla D**, **Gizzi L**, **Tschapek M**, **Erlenwein J**, **Petzke F.** Reduced task-induced variations in the distribution of activity across back muscle regions in individuals with low back pain. *Pain* 155: 944–953, 2014. doi:10.1016/j.pain.2014.01.027.
24. **Sanderson A**, **Cescon C**, **Heneghan NR**, **Kuithan P**, **Martinez-Valdes E**, **Rushton A**, **Barbero M**, **Falla D.** People with low back pain display a different distribution of erector spinae activity during a singular mono-planar lifting task. *Front Sports Act Living* 1: 65, 2019. doi:10.3389/fspor.2019.00065.
25. **Farina D**, **Gazzoni M**, **Merletti R.** Assessment of low back muscle fatigue by surface EMG signal analysis: methodological aspects. *J Electromyogr Kinesiol* 13: 319–332, 2003. doi:10.1016/s1050-6411(03)00040-3.
26. **Shiraishi M**, **Masuda T**, **Sadoyama T**, **Okada M.** Innervation zones in the back muscles investigated by multichannel surface EMG. *J Electromyogr Kinesiol* 5: 161–167, 1995. doi:10.1016/1050-6411(95)00002-h.
27. **van Helden JFL**, **Martinez-Valdes E**, **Strutton PH**, **Falla D**, **Chiou SY.** Reliability of high-density surface electromyography for assessing characteristics of the thoracic erector spinae during static and dynamic tasks. *J Electromyogr Kinesiol* 67: 102703, 2022. doi:10.1016/j.jelekin.2022.102703.
28. **Hodges P**, **Cresswell A**, **Thorstensson A.** Preparatory trunk motion accompanies rapid upper limb movement. *Exp Brain Res* 124: 69–79, 1999. doi:10.1007/s002210050601.
29. **Gabison S**, **Verrier MC**, **Nadeau S**, **Gagnon DH**, **Roy A**, **Flett HM.** Trunk strength and function using the multidirectional reach distance in individuals with non-traumatic spinal cord injury. *J Spinal Cord Med* 37: 537–547, 2014. doi:10.1179/2045772314Y.0000000246.
30. **Kanekar N**, **Aruin AS.** Aging and balance control in response to external perturbations: role of anticipatory and compensatory postural mechanisms. *Age (Dordr)* 36: 9621, 2014. doi:10.1007/s11357-014-9621-8.
31. **Field-Fote EC**, **Ray SS.** Seated reach distance and trunk excursion accurately reflect dynamic postural control in individuals with motor-incomplete spinal cord injury. *Spinal Cord* 48: 745–749, 2010. doi:10.1038/sc.2010.11.
32. **Martinez-Valdes E**, **Wilson F**, **Fleming N**, **McDonnell SJ**, **Horgan A**, **Falla D.** Rowers with a recent history of low back pain engage different regions of the lumbar erector spinae during rowing. *J Sci Med Sport* 22: 1206–1212, 2019. doi:10.1016/j.jsams.2019.07.007.
33. **Merletti R**, **Cerone GL.** Tutorial. Surface EMG detection, conditioning and pre-processing: best practices. *J Electromyogr Kinesiol* 54: 102440, 2020. doi:10.1016/j.jelekin.2020.102440.
34. **Vieira TM**, **Merletti R**, **Mesin L.** Automatic segmentation of surface EMG images: improving the estimation of neuromuscular activity. *J Biomech* 43: 2149–2158, 2010. doi:10.1016/j.jbiomech.2010.03.049.
35. **Hodges PW**, **Richardson CA.** Relationship between limb movement speed and associated contraction of the trunk muscles. *Ergonomics* 40: 1220–1230, 1997. doi:10.1080/001401397187469.
36. **Hodges PW**, **Bui BH.** A comparison of computer-based methods for the determination of onset of muscle contraction using electromyography. *Electroencephalogr Clin Neurophysiol* 101: 511–519, 1996. doi:10.1016/s0013-4694(96)95190-5.
37. **Hall L**, **Tsao H**, **MacDonald D**, **Coppieters M**, **Hodges PW.** Immediate effects of co-contraction training on motor control of the trunk muscles in people with recurrent low back pain. *J Electromyogr Kinesiol* 19: 763–773, 2009. doi:10.1016/j.jelekin.2007.09.008.
38. **Tsao H**, **Galea MP**, **Hodges PW.** How fast are feedforward postural adjustments of the abdominal muscles? *Behav Neurosci* 123: 687–693, 2009. doi:10.1037/a0015593.
39. **Kaewmanee T**, **Liang H**, **Aruin AS.** Effect of predictability of the magnitude of a perturbation on anticipatory and compensatory postural adjustments. *Exp Brain Res* 238: 2207–2219, 2020. doi:10.1007/s00221-020-05883-y.
40. **Chiou SY**, **Strutton PH**, **Perez MA.** Crossed corticospinal facilitation between arm and trunk muscles in humans. *J Neurophysiol* 120: 2595–2602, 2018. doi:10.1152/jn.00178.2018.
41. **Davey NJ**, **Lisle RM**, **Loxton-Edwards B**, **Nowicky AV**, **McGregor AH.** Activation of back muscles during voluntary abduction of the contralateral arm in humans. *Spine (Phila Pa 1976)* 27: 1355–1360, 2002. doi:10.1097/00007632-200206150-00019.
42. **Huang C**, **Klein CS**, **Meng Z**, **Zhang Y**, **Li S**, **Zhou P.** Innervation zone distribution of the biceps brachii muscle examined using voluntary and electrically-evoked high-density surface EMG. *J Neuroeng Rehabil* 16: 73, 2019. doi:10.1186/s12984-019-0544-6.
43. **Schlink BR**, **Nordin AD**, **Ferris DP.** Human myoelectric spatial patterns differ among lower limb muscles and locomotion speeds. *Physiol Rep* 8: e14652, 2020. doi:10.14814/phy2.14652.
44. **Aruin AS**, **Latash ML.** Directional specificity of postural muscles in feed-forward postural reactions during fast voluntary arm movements. *Exp Brain Res* 103: 323–332, 1995. doi:10.1007/BF00231718.
45. **Massion J.** Movement, posture and equilibrium interaction and coordination. *Prog Neurobiol* 38: 35–56, 1992. doi:10.1016/0301-0082(92)90034-c.
46. **Friedli WG**, **Cohen L**, **Hallett M**, **Stanhope S**, **Simon S.** Postural adjustments associated with rapid voluntary arm movements. II. Biomechanical analysis. *J Neurol Neurosurg Psychiatry* 51: 232–243, 1988. doi:10.1136/jnnp.51.2.232.
47. **Rowland RS**, **Jenkinson N**, **Chiou SY.** Age-related differences in corticospinal excitability and anticipatory postural adjustments of the trunk. *Front Aging Neurosci* 13: 718784, 2021. doi:10.3389/fnagi.2021.718784.
48. **Alexandrov AV**, **Frolov AA**, **Horak FB**, **Carlson-Kuhta P**, **Park S.** Feedback equilibrium control during human standing. *Biol Cybern* 93: 309–322, 2005. doi:10.1007/s00422-005-0004-1.
49. **Triolo RJ**, **Bailey SN**, **Miller ME**, **Lombardo LM**, **Audu ML.** Effects of stimulating hip and trunk muscles on seated stability, posture, and reach after spinal cord injury. *Arch Phys Med Rehabil* 94: 1766–1775, 2013. doi:10.1016/j.apmr.2013.02.023.
50. **Eginyan G**, **Williams AMM**, **Joseph KS**, **Lam T.** Trunk muscle activity and kinematics during boxing and battle rope exercise in people

Downloaded from journals.physiology.org/journal/jn at Imperial Col London (2A0C:5BC0:0040:1008:1A60:24FF:FEA6:CAE5) on July 16, 2025.

with motor-complete spinal cord injury. *J Spinal Cord Med* 47: 135–142, 2024. doi:10.1080/10790268.2021.2005993.
51. **O'Sullivan PB**, **Dankaerts W**, **Burnett AF**, **Farrell GT**, **Jefford E**, **Naylor CS**, **O'Sullivan KJ.** Effect of different upright sitting postures on spinal-pelvic curvature and trunk muscle activation in a pain-free population. *Spine (Phila Pa 1976)* 31: E707–E712, 2006. doi:10.1097/01.brs.0000234735.98075.50.
52. **Takiguchi M**, **Miyashita K**, **Yamazaki K**, **Funakoshi K.** Chondroitinase ABC administration facilitates serotonergic innervation of motoneurons in rats with complete spinal cord transection. *Front Integr Neurosci* 16: 881632, 2022. doi:10.3389/fnint.2022.881632.
53. **Bareyre FM**, **Kerschensteiner M**, **Raineteau O**, **Mettenleiter TC**, **Weinmann O**, **Schwab ME.** The injured spinal cord spontaneously forms a new intraspinal circuit in adult rats. *Nat Neurosci* 7: 269–277, 2004. doi:10.1038/nn1195.
54. **Bunday KL**, **Oudega M**, **Perez MA.** Aberrant crossed corticospinal facilitation in muscles distant from a spinal cord injury. *PLoS One* 8: e76747, 2013. doi:10.1371/journal.pone.0076747.
55. **Bjerkefors A**, **Carpenter MG**, **Cresswell AG**, **Thorstensson A.** Trunk muscle activation in a person with clinically complete thoracic spinal cord injury. *J Rehabil Med* 41: 390–392, 2009. doi:10.2340/16501977-0336.
56. **Fox EJ**, **Tester NJ**, **Kautz SA**, **Howland DR**, **Clark DJ**, **Garvan C**, **Behrman AL.** Modular control of varied locomotor tasks in children with incomplete spinal cord injuries. *J Neurophysiol* 110: 1415–1425, 2013. doi:10.1152/jn.00676.2012.
57. **Hayes HB**, **Chvatal SA**, **French MA**, **Ting LH**, **Trumbower RD.** Neuromuscular constraints on muscle coordination during overground walking in persons with chronic incomplete spinal cord injury. *Clin Neurophysiol* 125: 2024–2035, 2014. doi:10.1016/j.clinph.2014.02.001.
58. **Chvatal SA**, **Macpherson JM**, **Torres-Oviedo G**, **Ting LH.** Absence of postural muscle synergies for balance after spinal cord transection. *J Neurophysiol* 110: 1301–1310, 2013. doi:10.1152/jn.00038.2013.
59. **Hart CB**, **Giszter SF.** Modular premotor drives and unit bursts as primitives for frog motor behaviors. *J Neurosci* 24: 5269–5282, 2004. doi:10.1523/JNEUROSCI.5626-03.2004.
60. **Milosevic M**, **Masani K**, **Wu N**, **McConville KM**, **Popovic MR.** Trunk muscle co-activation using functional electrical stimulation modifies center of pressure fluctuations during quiet sitting by increasing trunk stiffness. *J Neuroeng Rehabil* 12: 99, 2015. doi:10.1186/s12984-015-0091-8.
61. **Falla D**, **Farina D.** Periodic increases in force during sustained contraction reduce fatigue and facilitate spatial redistribution of trapezius muscle activity. *Exp Brain Res* 182: 99–107, 2007. doi:10.1007/s00221-007-0974-4.
62. **Watanabe K**, **Kouzaki M**, **Moritani T.** Regional neuromuscular regulation within human rectus femoris muscle during gait. *J Biomech* 47: 3502–3508, 2014. doi:10.1016/j.jbiomech.2014.09.001.
63. **de Souza LM**, **da Fonseca DB**, **Cabral HD**, **de Oliveira LF**, **Vieira TM.** Is myoelectric activity distributed equally within the rectus femoris muscle during loaded, squat exercises? *J Electromyogr Kinesiol* 33: 10–19, 2017. doi:10.1016/j.jelekin.2017.01.003.
64. **Hagio S**, **Fukuda M**, **Kouzaki M.** Identification of muscle synergies associated with gait transition in humans. *Front Hum Neurosci* 9: 48–12, 2015. doi:10.3389/fnhum.2015.00048.
65. **Farina D.** Interpretation of the surface electromyogram in dynamic contractions. *Exerc Sport Sci Rev* 34: 121–127, 2006. doi:10.1249/00003677-200607000-00006.
66. **Davey NJ**, **Smith HC**, **Savic G**, **Maskill DW**, **Ellaway PH**, **Frankel HL.** Comparison of input-output patterns in the corticospinal system of normal subjects and incomplete spinal cord injured patients. *Exp Brain Res* 127: 382–390, 1999. doi:10.1007/s002210050806.
67. **Moore CD**, **Craven BC**, **Thabane L**, **Laing AC**, **Frank-Wilson AW**, **Kontulainen SA**, **Papaioannou A**, **Adachi JD**, **Giangregorio LM.** Lower-extremity muscle atrophy and fat infiltration after chronic spinal cord injury. *J Musculoskelet Neuronal Interact* 15: 32–41, 2015.
68. **Giangregorio L**, **McCartney N.** Bone loss and muscle atrophy in spinal cord injury: epidemiology, fracture prediction, and rehabilitation strategies. *J Spinal Cord Med* 29: 489–500, 2006. doi:10.1080/10790268.2006.11753898.
69. **Bunge RP**, **Puckett WR**, **Becerra JL**, **Marcillo A**, **Quencer RM.** Observations on the pathology of human spinal cord injury. A review and classification of 22 new cases with details from a case of chronic cord compression with extensive focal demyelination. *Adv Neurol* 59: 75–89, 1993.
70. **Thomas CK**, **Bakels R**, **Klein CS**, **Zijdewind I.** Human spinal cord injury: motor unit properties and behaviour. *Acta Physiol (Oxf)* 210: 5–19, 2014. doi:10.1111/apha.12153.
71. **Castillo-Escario Y**, **Kumru H**, **Valls-Sole J**, **Garcia-Alen L**, **Jane R**, **Vidal J.** Quantitative evaluation of trunk function and the StartReact effect during reaching in patients with cervical and thoracic spinal cord injury. *J Neural Eng* 18: 0460d2, 2021. doi:10.1088/1741-2552/ac19d3.
72. **Wang YJ**, **Li JJ**, **Zhou HJ**, **Liu GL**, **Zheng Y**, **Wei B**, **Zhang Y**, **Hao CX**, **Kang HQ**, **Yuan Y**, **Gao LJ.** Surface electromyography as a measure of trunk muscle activity in patients with spinal cord injury: a meta-analytic review. *J Spinal Cord Med* 39: 15–23, 2016. doi:10.1179/2045772315Y.0000000059.
73. **Seelen HA**, **Vuurman EF.** Compensatory muscle activity for sitting posture during upper extremity task performance in paraplegic persons. *Scand J Rehabil Med* 23: 89–96, 1991.
74. **Seelen HAM**, **Potten YJM**, **Huson A**, **Spaans F**, **Reulen JPH.** Impaired balance control in paraplegic subjects. *J Electromyogr Kinesiol* 7: 149–160, 1997. doi:10.1016/s1050-6411(97)88884-0.
75. **McGorry RW**, **Hsiang SM**, **Fathallah FA**, **Clancy EA.** Timing of activation of the erector spinae and hamstrings during a trunk flexion and extension task. *Spine (Phila Pa 1976)* 26: 418–425, 2001. doi:10.1097/00007632-200102150-00019.
76. **Vera-Garcia FJ**, **Brown SH**, **Gray JR**, **McGill SM.** Effects of different levels of torso coactivation on trunk muscular and kinematic responses to posteriorly applied sudden loads. *Clin Biomech (Bristol)* 21: 443–455, 2006. doi:10.1016/j.clinbiomech.2005.12.006.
77. **Louis N**, **Gorce P.** Surface electromyography activity of upper limb muscle during wheelchair propulsion: influence of wheelchair configuration. *Clin Biomech (Bristol)* 25: 879–885, 2010. doi:10.1016/j.clinbiomech.2010.07.002.
78. **Chow JW**, **Millikan TA**, **Carlton LG**, **Chae WS**, **Lim YT**, **Morse MI.** Kinematic and electromyographic analysis of wheelchair propulsion on ramps of different slopes for young men with paraplegia. *Arch Phys Med Rehabil* 90: 271–278, 2009. doi:10.1016/j.apmr.2008.07.019.
79. **Desroches G**, **Gagnon D**, **Nadeau S**, **Popovic M.** Magnitude of forward trunk flexion influences upper limb muscular efforts and dynamic postural stability requirements during sitting pivot transfers in individuals with spinal cord injury. *J Electromyogr Kinesiol* 23: 1325–1333, 2013. doi:10.1016/j.jelekin.2013.09.003.
80. **Jordanic M**, **Rojas-Martinez M**, **Mananas MA**, **Alonso JF.** Prediction of isometric motor tasks and effort levels based on high-density EMG in patients with incomplete spinal cord injury. *J Neural Eng* 13: 046002, 2016. doi:10.1088/1741-2560/13/4/046002.
81. **Zhang X**, **Li X**, **Tang X**, **Chen X**, **Chen X**, **Zhou P.** Spatial filtering for enhanced high-density surface electromyographic examination of neuromuscular changes and its application to spinal cord injury. *J Neuroeng Rehabil* 17: 160, 2020. doi:10.1186/s12984-020-00786-z.
82. **Pilkar R**, **Momeni K**, **Ramanujam A**, **Ravi M**, **Garbarini E**, **Forrest GF.** Use of surface EMG in clinical rehabilitation of individuals with SCI: barriers and future considerations. *Front Neurol* 11: 578559, 2020. doi:10.3389/fneur.2020.578559.
83. **Korupolu R**, **Stampas A**, **Singh M**, **Zhou P**, **Francisco G.** Electrophysiological outcome measures in spinal cord injury clinical trials: a systematic review. *Top Spinal Cord Inj Rehabil* 25: 340–354, 2019. doi:10.1310/sci2504-340.
84. **Singh A**, **Tetreault L**, **Kalsi-Ryan S**, **Nouri A**, **Fehlings MG.** Global prevalence and incidence of traumatic spinal cord injury. *Clin Epidemiol* 6: 309–331, 2014. doi:10.2147/CLEP.S68889.
85. **Pradhan A**, **Malagon G**, **Lagacy R**, **Chester V**, **Kuruganti U.** Effect of age and sex on strength and spatial electromyography during knee extension. *J Physiol Anthropol* 39: 11, 2020. doi:10.1186/s40101-020-00219-9.
86. **Taylor CA**, **Kopicko BH**, **Negro F**, **Thompson CK.** Sex differences in the detection of motor unit action potentials identified using high-density surface electromyography. *J Electromyogr Kinesiol* 65: 102675, 2022. doi:10.1016/j.jelekin.2022.102675.
87. **Clark BC**, **Manini TM**, **Thé DJ**, **Doldo NA**, **Ploutz-Snyder LL.** Gender differences in skeletal muscle fatigability are related to contraction type and EMG spectral compression. *J Appl Physiol (1985)* 94: 2263–2272, 2003. doi:10.1152/japplphysiol.00926.2002.

Downloaded from journals.physiology.org/journal/jn at Imperial Col London (2A0C:5BC0:0040:1008:1A60:24FF:FEA6:CAE5) on July 16, 2025.

88. **Pincivero DM**, **Gear WS**, **Sterner RL**, **Karunakara RG.** Gender differences in the relationship between quadriceps work and fatigue during high-intensity exercise. *J Strength Cond Res* 14: 202–206, 2000. doi:10.1519/1533-4287(2000)014<0202:GDITRB>2.0.CO;2.
89. **Kavanagh JJ**, **Smith KA**, **Minahan CL.** Sex differences in muscle activity emerge during sustained low-intensity contractions but not during intermittent low-intensity contractions. *Physiol Rep* 8: e14398, 2020. doi:10.14814/phy2.14398.
90. **Gagnon D**, **Nadeau S**, **Gravel D**, **Noreau L**, **Lariviere C**, **Gagnon D.** Biomechanical analysis of a posterior transfer maneuver on a level surface in individuals with high and low-level spinal cord injuries. *Clin Biomech (Bristol)* 18: 319–331, 2003. doi:10.1016/s0268-0033(03)00016-0.

Downloaded from journals.physiology.org/journal/jn at Imperial Col London (2A0C:5BC0:0040:1008:1A60:24FF:FEA6:CAE5) on July 16, 2025.